Analysis of the temperature and excitation intensity dependencies of photoluminescence in undoped GaN films

M. A. Reshchikov* and R. Y. Korotkov
Department of Materials Sciences and Engineering, Northwestern University, Evanston, Illinois 60208
(Received 15 March 2001; revised manuscript received 14 June 2001; published 29 August 2001)

Steady-state photoluminescence (PL) from undoped wurtzite GaN has been studied in detail over a wide range of temperatures and excitation intensities. Both the observed steps in the temperature dependence of the PL intensity, and the nonlinear dependence of the PL intensity on excitation power for different PL bands are quantitatively explained by competition between different recombination channels. Hole-capture cross sections, defect concentrations, and thermal activation energies of the main acceptors in undoped GaN are estimated from the analysis of temperature and excitation intensity dependencies of the PL.

DOI: 10.1103/PhysRevB.64.115205 PACS number(s): 61.72.Ji, 78.55.Cr, 71.55.Eq

I. INTRODUCTION

Photoluminescence (PL) spectroscopy is widely used to qualitatively characterize GaN and its alloys. However, quantitative studies of point defects by PL are rarely undertaken. For example, to the best of our knowledge, no direct information about the defect concentrations has been obtained from PL studies in GaN. Often, a qualitative estimation of the acceptor concentration in *n*-type GaN is made by comparing the ratios between the defect and near-band-edge emission intensities.[1,2] However, this ratio is shown to depend not only on the defect concentration but also on experimental conditions, in particular on excitation intensity.[3,4] Temperature dependence of the defect-related PL intensity is typically used to determine the nature of an optical transition. For example, one would differentiate between donor-acceptor pair (DAP) transitions and the conduction band-acceptor (eA) transitions by the temperature behavior of PL.[5–7] However, the temperature behavior of PL may be complicated by a competition between several recombination channels as will be shown below. On the other hand, the complex dependencies of the PL spectrum on temperature and on excitation intensity can provide important information on characteristics of point defects and carrier kinetics in the semiconductor.

A typical PL spectrum of undoped wurtzite GaN exhibits a yellow luminescence (YL) band with a maximum at about 2.2 eV, a shallow donor–shallow acceptor (SD-SA) band with the main peak at 3.27 eV, and often a blue luminescence (BL) band with a maximum at about 2.9 eV.[8–10] The assignment of these PL bands to specific radiative transitions is controversial, yet it was proposed that gallium vacancy (V_{Ga}) may be involved. An isolated V_{Ga} and its complexes with shallow donors or with hydrogen are characterized by low formation energies and expected to be multiple-charged acceptors in *n*-type GaN.[11–13] One of the distinguished features of the charged defects is a large capture cross section for the carriers with opposite sign.[14] To the best of our knowledge, the only estimate of the hole-capture cross section in undoped GaN has been made for the YL-related defect by the photoinduced current transient spectroscopy (PICTS) method.[15] The hole-capture cross sections for other defects in undoped *n*-type GaN remain unknown. In this work we have obtained the hole-capture cross sections for the main radiative defects in undoped GaN. For this, a detailed balance of carriers in *n*-type semiconductor at different PL conditions has been considered phenomenologically. Acceptor concentrations, the minority carrier lifetimes, and the internal quantum efficiency (QE) of PL have also been estimated for the studied samples. The paper is comprised of five sections.

In Sec. II we derive a general expression for the defect-related PL intensity in the presence of several defects at an arbitrary temperature. Section II A is limited to the low excitation intensity case. Previously, a similar approach to the analysis of PL has been presented for the specific defects in GaAs and can be found in Refs. 16 and 17. A much-simplified consideration of the carrier balance in GaN has been reported in Refs. 3, 4, and 18. Section II B describes the excitation power dependence of the PL intensity. The concentration of the radiative defects is estimated from these dependencies. The experimental results chosen to provide a quantitative comparison to the theory are presented and discussed in Secs. III and IV. In Sec. V the main conclusions of the paper are presented.

II. THEORY

A. Temperature dependence of PL intensity

Unintentionally doped GaN contains shallow donors D and several acceptors A_i with concentrations N_D and N_{Ai}, respectively. In *n*-type GaN the Fermi level is close to the conduction band. Thus all acceptors are ionized and there are no holes in the valence band under equilibrium conditions at low temperature. The nonequilibrium electron-hole pairs are excited with a generation rate G ($\mathrm{cm^{-3}\,s^{-1}}$). The concentration of photogenerated holes in the valence band is p, the concentration of equilibrium (n_0), and photogenerated (δn) free electrons is $n=n_0+\delta n$. After optical excitation, the holes are captured by acceptors with the rate $C_{pi}N_{Ai}^{-}p$, where C_{pi} ($\mathrm{cm^3\,s^{-1}}$) is the hole-capture coefficient for the ith acceptor and N_{Ai}^{-} is the concentration of ionized acceptors of i type. A competing process is the formation of excitons with the rate $C_{\mathrm{ex}}np$, where coefficient C_{ex} describes the efficiency

of the exciton formation. Some of the holes recombine nonradiatively. We will introduce for simplicity the nonradiative recombination rate as $C_{ps}N_S^- p$, where C_{ps} and N_S^- are the average hole-capture coefficient and the concentration of nonradiative centers, respectively. Thus the hole-capture rate can be expressed in general as $C_i N_i^- p$ where $C_i = C_{\rm ex}$, C_{pi}, or C_{ps} and $N_i^- = n$, N_{Ai}^-, or N_S^- for excitons, radiative, and nonradiative defects, respectively.

Holes captured by defects or excitons may return to the valence band as a result of thermal activation or exciton dissociation. The probability of this process, Q_i, at temperature T is proportional to $\exp(-E_i/k_BT)$, where E_i is the thermal activation energy of the radiative acceptors (E_{Ai}), nonradiative defects (E_S), or the exciton dissociation energy ($E_{\rm ex}$) and k_B is the Boltzmann's constant. Taking into account all these processes, the detailed balance equation for the hole concentration in the valence band in a steady state and in the case of N recombination channels can be written in the form

$$\frac{\partial p}{\partial t} = G - \sum_{i=1}^{N} C_i N_i^- p + \sum_{i=1}^{N} Q_i N_i^0 = 0, \tag{1}$$

where $N_i^0 = N_{Ai}^0$, N_S^0, and $N_{\rm ex}$ are the concentration of holes bound to radiative acceptors, nonradiative centers and excitons, respectively.[19] Only the case of low excitation intensity, $N_i^0 \ll N_i^- \approx N_i$, will be considered in this section, while the following section is devoted to the analysis of the PL intensity at high excitation intensities.

In this study, it is assumed that the capture rates are much faster than recombination rates, which will be supported below by experimental results. As a result, efficiency of each recombination channel is proportional to the rate of capture of the minority carriers (holes in n-type GaN). Therefore the low-temperature QE of each recombination channel $\eta_i(0)$ is given by the ratio of hole capture rate of a specific channel to the total escape rate of holes from the valence band under the approximation that both the thermal release of the bound holes and the exciton dissociation are negligible:

$$\eta_i(0) = \frac{C_i N_i p}{\sum_{j=1}^{N} C_j N_j p} = \frac{C_i N_i}{\sum_{j=1}^{N} C_j N_j}. \tag{2}$$

The steady-state equation for the concentration of holes bound to the ith defect in the general case is

$$\frac{\partial N_i^0}{\partial t} = C_i N_i p - \frac{N_i^0}{\tau_{Ri}} - Q_i N_i^0 = 0, \tag{3}$$

where the second term in Eq. (3) describes recombination via the ith channel and the parameter τ_{Ri} characterizes the recombination lifetime (in the general case it may vary with time in transient processes). Rearranging Eqs. (1)–(3) one can arrive at the following equation for the concentration of holes bound to the ith acceptor N_i^0:

$$N_i^0 = \frac{\eta_i(0)\left(G + \sum_{j=1}^{N} Q_j N_j^0 \right)}{\tau_{Ri}^{-1} + Q_i}. \tag{4}$$

By solving the linear system of Eq. (4) for the unknown parameters N_i^0, we finally obtain an expression for the intensity of PL via each defect,

$$I_i^{\rm PL} = \frac{N_i^0}{\tau_{Ri}} = \frac{\eta_i}{1 + (1-\eta_i)\tau_{Ri} Q_i} G, \tag{5}$$

where

$$\eta_i = \eta_i(0)\left(1 - \sum_{j \neq i}^{N} \frac{\eta_j(0)\tau_{Rj} Q_j}{1 + \tau_{Rj} Q_j} \right)^{-1}. \tag{6}$$

The term in front of G in Eq. (5) is the actual QE of the ith channel, that accounts for the dissociation of excitons and thermal escape of holes from the defects to the valence band. It is evident from Eqs. (5) and (6) that the temperature dependence of the PL intensity is largely determined by exciton dissociation and thermal escape of holes from defects to the valence band. Exact expressions for the exciton dissociation, considering both free and bound excitons, may be found elsewhere.[20] This work is devoted to the analysis of the defect-related PL, and for simplicity, we can determine the effect of the exciton dissociation on the balance of carriers from the experiment. Indeed, since the exciton dissociation occurs at lower temperatures than the hole thermalization from acceptor levels, the term $\tau_{Ri} Q_i$ for the exciton recombination can be expressed from Eqs. (5) and (6) as

$$\tau_{R\rm ex} Q_{\rm ex} = \frac{\eta_{\rm ex}(0) G - I_{\rm ex}^{\rm PL}}{[1 - \eta_{\rm ex}(0)] I_{\rm ex}^{\rm PL}}, \tag{7}$$

where $I_{\rm ex}^{\rm PL}$ is the integrated PL intensity in exciton region of the spectrum, which can be found experimentally.

The probability of thermal activation of holes from an acceptor can be obtained from a detailed balance consideration:

$$Q_i = C_{pi} g^{-1} N_v \exp\left(-\frac{E_{Ai}}{k_B T} \right) \tag{8}$$

with

$$N_v = 2\left(\frac{m_h k_B T}{2\pi\hbar^2} \right)^{3/2} \tag{9}$$

and

$$C_{pi} = \sigma_{pi} v_p = \sigma_{pi} \sqrt{\frac{8 k_B T}{\pi m_h}}, \tag{10}$$

where g is the degeneracy factor of the acceptor level, N_v is the density of states in the valence band, m_h is the effective mass of the holes in the valence band, v_p is their thermal velocity, and σ_{pi} is, by definition, the hole-capture cross section of the ith acceptor. Analysis of Eqs. (5) and (8) shows

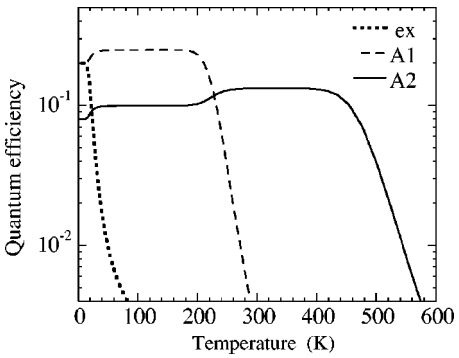

FIG. 1. Calculated temperature dependencies of the QE for three radiative recombination channels in GaN: excitonic (ex) and via two acceptors ($A1$ and $A2$). The dependencies were calculated using Eqs. (5)–(8) with the following parameters: $\eta_{ex}(0)=0.2$, $\eta_{A1}(0)=0.2$, $\eta_{A2}(0)=0.08$; $\tau_{Rex}Q_{ex}=250\exp(-10\ \mathrm{meV}/k_BT)$, $\tau_{R1}=10^{-5}$ s, $\tau_{R2}=5\times10^{-5}$ s, $C_{p1}=10^{-6}$ cm^3 s^{-1}, $C_{p2}=4\times10^{-7}$ cm^3 s^{-1}, $E_{A1}=0.34$ eV, $E_{A2}=0.8$ eV.

that the temperature dependence of PL intensity for the ith acceptor involves a region of thermal quenching with an activation energy E_{Ai} at temperatures T satisfying the condition $(1-\eta_i)\tau_{Ri}Q_i>1$. Variation of the parameter η_i in this region of thermal quenching of PL via the ith acceptor can be ignored if the quenching regions of different defects do not overlap significantly. The parameters of the ith acceptor, E_{Ai} and C_{pi} (or σ_{pi}), can be obtained by fitting Eq. (5) to the experimental dependence of the PL intensity in the region of thermal quenching of the PL band related to the ith acceptor. Note that the value of E_{Ai} calculated from the fit to the experimental dependence using Eq. (5) is somewhat different from the ionization energy obtained from the slope of the Arrhenius plot of the $I^{\mathrm{PL}}(T^{-1})$ due to temperature dependence of N_v and C_{pi}. Furthermore, capture cross sections of some defects can be thermally activated, leading to a difference between the actual thermal depth of the acceptor and the experimentally found value of E_{Ai}.

Analysis of Eqs. (5)–(10) suggests that the integrated PL intensity of the given recombination channel at a given temperature depends on the quenching state of the rest of the channels. Therefore several increases of the PL intensity in the $I^{\mathrm{PL}}(T)$ dependence are expected in the form of intensity steps corresponding to thermal quenching of other PL bands. An example of the calculated temperature dependencies of PL intensity for three radiative recombination channels in GaN is shown in Fig. 1. The increase in PL intensity in the region of thermal quenching of one of the recombination channels is associated with redistribution of the released holes among all unquenched channels. The total quenching of the ith channel results in the stepwise increase of the recombination intensity of unquenched channels by R_i times if the overlap of the quenching regions can be neglected. A simple expression for R_i can be obtained from Eqs. (5) and (6):

$$R_i \approx 1+\frac{\eta_i(0)}{1-\sum_j \eta_j(0)}, \tag{11}$$

where the summation is taken over the channels which have been thermally quenched prior to the quenching of the ith channel.

The QE of PL can be found from the temperature dependence of PL intensity using Eq. (11). First, the *relative* values of parameters $\eta_i(0)$ for all PL bands are obtained at low temperature, when the dissociation of excitons and thermal release of holes from acceptors are assumed to be negligible. Indeed, from Eq. (5) with $Q_i, Q_j=0$ the integrated intensity of PL via ith defect is

$$I_i^{\mathrm{PL}}=\eta_i(0)G. \tag{12}$$

Then, according to Eqs. (11) and (12), the *absolute* value of $\eta_i(0)$ can be calculated from the value of the step in PL intensity for any band, which is related to the thermal quenching of the ith channel:

$$\eta_i(0)=\left(\frac{1}{R_i-1}+\frac{\sum_j I_j^{\mathrm{PL}}(0)}{I_i^{\mathrm{PL}}(0)}\right)^{-1}, \tag{13}$$

where the summation is taken over the channels quenched prior to quenching of the ith channel.

B. Dependence of PL intensity on excitation power

In the previous section, a possible saturation of the defect-related PL was ignored when we assumed that $N_i^0 \ll N_i$. However, high and even moderate excitation power can saturate the defect-related PL intensity since the defect concentration and lifetime are finite. Let us consider the case when the thermalization of the holes trapped by the ith acceptor is negligible and assume that only the ith acceptor is subject to saturation by nonequilibrium holes in the considered excitation range. Then, the steady-state rate equations for the holes in the valence band and at the ith acceptor [Eqs. (1) and (3)] can be rewritten in the form

$$\frac{\partial p}{\partial t}=G+\frac{pN_i^0}{\tau_i N_i}-\frac{p}{\tau^*}=0, \tag{14}$$

$$\frac{\partial N_i^0}{\partial t}=\frac{p}{\tau_i}\left(1-\frac{N_i^0}{N_i}\right)-\frac{N_i^0}{\tau_{Ri}}=0. \tag{15}$$

Here, τ_i is a characteristic time of the hole capture by the ith acceptor and τ^* is a lifetime of holes in the valence band:

$$\tau_i=(C_{pi}N_i)^{-1}, \tag{16}$$

$$\tau^*=\left(\sum_{j=k}^{N} C_jN_j\right)^{-1}, \tag{17}$$

where the summation is taken over all channels except the quenched $(k-1)$ ones. Note that $\eta_i=\tau^*/\tau_i$ is the QE of PL via ith acceptor at low excitation intensity and arbitrary temperature, when the quenching of the ith acceptor is negligible. A solution of Eqs. (14) and (15) has the form

$$N_i^0=\frac{1}{2}N_i(K_i+\eta_i^{-1})-N_i\sqrt{\frac{(K_i+\eta_i^{-1})^2}{4}-K_i} \quad (18)$$

with $K_i=G\tau_{Ri}/N_i$.

For the case of low QE of the ith channel, $\eta_i \ll 1$, Eq. (18) can be expanded using the Taylor series:

$$I_i^{\mathrm{PL}}=\frac{N_i^0}{\tau_{Ri}}\approx G\left(\frac{G\tau_{Ri}}{N_i}+\frac{1}{\eta_i}\right)^{-1}. \quad (19)$$

At low excitation rate ($G\tau_{Ri}\eta_i \ll N_i$) this dependence is linear, and at high excitation rate it is expected to saturate at the value of $N_i\tau_{Ri}^{-1}$. Under saturated conditions of PL, the temperature dependence of I_i^{PL} has no steps in its low-temperature part since the saturated acceptors cannot capture holes released from other channels. For the same reason, the thermal quenching at high excitation intensities starts at higher temperatures than for the low excitation power conditions.

Instead of complete saturation, a nearly square-root dependence of the PL intensity has been observed at room temperature for excitation densities higher than 10^{-2} W/cm^2 in our samples. Similar results have been presented in Ref. 4. The square-root dependence of the defect-related PL intensity as a function of excitation power may be observed at high excitation density when the concentration of the photoexcited carriers (δn and p) exceeds the free electron concentration in the dark (n_0).[4] This leads to a decrease in the lifetime of the defect-related recombination. However, the excitation density necessary to inject $\delta n \sim 10^{18}$ cm^{-3} (typical concentration of free electrons at room temperature) nonequilibrium carriers, is about 10^5 W/cm^2 in GaN.[21] To the best of our knowledge, the square-root dependence of the defect-related PL with excitation power in the range $\sim 10^{-2}$–10^2 W/cm^2 remains unexplained for the observed excitation powers.[22]

As an alternative explanation of the observed effect, we propose that the recombination through deep nonradiative donors (traps for the holes) is responsible for the ($\delta n \gg n_0$) condition in n-type GaN, at least at room temperature, such that at moderate excitation levels the concentration of free electrons can increase due to filling of nonradiative donors with photogenerated holes, thus leading to a square-root dependence of the defect-related PL intensity in this excitation range.

The balance equations for electrons in the conduction band and holes in the valence band in a steady state are

$$\frac{\partial n}{\partial t}=G-\sum_j C_{nj}N_{Aj}^0(n_0+\delta n)-C_{nS}N_{DS}^+(n_0+\delta n) - C_{\mathrm{ex}}p(n_0+\delta n)=0, \quad (20)$$

$$\frac{\partial p}{\partial t}=G-\sum_j C_{pj}N_{Aj}^-p-C_{pS}N_{DS}^0p-C_{\mathrm{ex}}p(n_0+\delta n)=0, \quad (21)$$

where C_{nj} and C_{nS} are electron-capture coefficients for the jth acceptor and nonradiative deep donor, respectively. In these expressions we ignored the DAP-type recombination at room temperature and separated the term accounting for recombination via nonradiative defects acting as deep donors with a concentration N_{DS}. Note that nonradiative acceptors, if present, can be included in the sum with radiative acceptors. Free excitons can be captured by nonradiative centers too, and this will just formally reduce the phenomenological parameter C_{ex}.

Furthermore, the balance should take place for each recombination channel. In particular,

$$C_{ni}N_{Ai}^0(n_0+\delta n)=C_{pi}N_{Ai}^-p, \quad (22)$$

$$C_{nS}N_{DS}^+(n_0+\delta n)=C_{pS}N_{DS}^0p. \quad (23)$$

Finally, the conservation of charge in n-type semiconductor can be added in the form

$$n_0+\delta n+\sum_j N_{Aj}^-=N_{DS}^++N_D^++p, \quad (24)$$

or

$$\delta n=\sum_j N_{Aj}^0+N_{DS}^++p, \quad (25)$$

where $N_{DS}^+=n_0+\Sigma_j N_{Aj}$ is the concentration of the ionized shallow donors.

The system of Eqs. (20)–(25) can be solved numerically and the dependencies of δn, p, N_{Ai}^0, and N_{DS}^+ on G can be found for the fixed parameters C_{ni}, C_{pi}, C_{nS}, C_{pS}, C_{ex}, N_{Ai}, N_{DS}, and n_0. At room temperature we can restrict our consideration to three recombination channels in n-type GaN: an excitonic (ex), radiative (i), and nonradiative (S) recombination, which is consistent with the observation of the near-band-gap and YL bands in the room-temperature PL spectrum.[4] In choosing the fixed parameters, we held the following in equations: $C_{pS}N_{DS} \gg C_{pi}N_{Ai}, C_{\mathrm{ex}}n_0$ (nonradiative recombination is dominant) and $C_{pi} \gg C_{ni}$, $C_{pS} \gg C_{nS}$ (preferential capture of holes by both radiative acceptors and nonradiative donors).

An example of numerical solution of the system of Eqs. (20), (22), (23), (25) for the above-mentioned three recombination channels is shown in Fig. 2. At low excitation intensity (region I), $\delta n \ll n_0$ and all variable parameters (p, N_{Ai}^0, N_{DS}^+, and δn) increase linearly with excitation rate: $p \approx G(C_{pS}N_{DS})^{-1}$, $N_{Ai}^0 \approx \eta_i(0)G(C_{ni}n_0)^{-1}$, and $N_{DS}^+ \approx \delta n \approx G(C_{nS}n_0)^{-1}$. Intensity of the defect-related PL equals $C_{ni}N_{Ai}^0(n_0+\delta n)$ and in this region it increases linearly with G. The PL intensity saturates when $N_{Ai}^0 \approx N_{Ai}$ (region II). The value of δn in our example increases mostly due to filling of nonradiative donors by holes and it exceeds n_0 at $G > C_{nS}n_0^2$ (region III). At $G > C_{nS}N_{DS}^2$, the nonradiative centers become nearly filled with holes ($N_{DS}^+ \approx N_{DS}$), and concentration of free electrons saturates at the value of $n_0+\delta n \approx N_{DS}$ (region IV). Finally, at $G > C_{ex}N_{DS}^2$, excitonic recombination becomes dominant and the concentration of free electrons increases again (region V). Interestingly, in the excitation range $C_{nS}N_{DS}^2 > G > C_{nS}n_0^2$, the concentration of

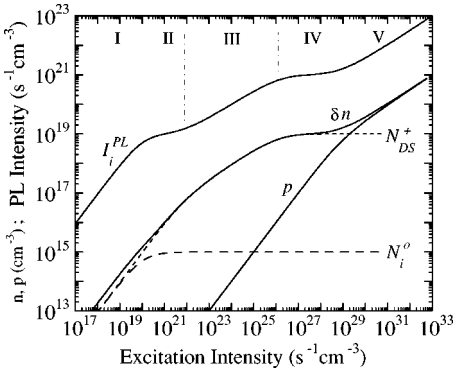

FIG. 2. Calculated defect-related PL intensity and concentrations of free and bound electrons and holes versus excitation intensity in GaN with three recombination mechanisms: excitonic (ex), nonradiative recombination via deep donors (S), and radiative recombination via acceptor (i). The dependencies were calculated numerically using Eqs. (20), (22), (23), and (25) with the following parameters: $n_0=10^{17}$ cm^{-3}, $N_{Ai}=10^{15}$ cm^{-3}, $N_{DS}=10^{19}$ cm^{-3}, $C_{nS}=10^{-12}$ cm^3 s^{-1}, $C_{pS}=10^{-9}$ cm^3 s^{-1}, $C_{ni}=10^{-13}$ cm^3 s^{-1}, $C_{pi}=10^{-6}$ cm^3 s^{-1}, $C_{\rm ex}=10^{-9}$ cm^3 s^{-1}. PL intensity is linear with G in region I, it saturates in regions II and IV and it follows the square-root dependence in regions III and V.

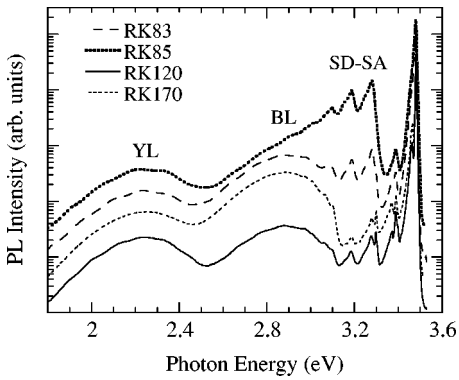

FIG. 3. PL spectra of undoped GaN samples at 15 K. Excitation density is 0.3 W/cm^2.

free electrons, as well as the concentration of holes bound to nonradiative donors, depends as a square root on excitation intensity:

$$n_0+\delta n\approx N_{DS}^{+}\approx\sqrt{\frac{G}{C_{nS}}}, \tag{26}$$

provided that $C_{nS}<C_{pS}$. Once the deep donors are saturated with holes, the excitonic (or band-to-band) transitions may become the dominant recombination mechanism, also giving the square-root dependence:

$$\delta n\approx p\approx\sqrt{\frac{G}{C_{\rm ex}}}. \tag{27}$$

The defect-related PL intensity follows variation of $(n_0+\delta n)$ when the defect is saturated with holes: $I_i^{\rm PL}=C_{ni}N_{Ai}(n_0+\delta n)$. Therefore, for relatively small C_{nS} and large N_{DS}, the defect-related PL intensity may follow the square-root dependence at moderate injections. The change of the dominant recombination mechanism from nonradiative to radiative would increase the lifetime of minority carriers and conserve the square-root dependence of the defect-related PL intensity on excitation intensity.

III. EXPERIMENTAL RESULTS

A. Experimental details

For the optical studies, we used GaN layers, about 2 μm thick, that were grown by metal organic vapor phase epitaxy on c-plane sapphire. The concentration of free electrons (n_0) and their mobility (μ_n), obtained from the Hall-effect measurements at room temperature, varied in the ranges $(1-7)\times10^{17}$ cm^{-3} and 300–500 cm^2 V^{-1} s^{-1}, respectively. Steady-state PL was excited with a continuous-wave (cw) He-Cd laser (photon energy 3.81 eV) in the reflection configuration, dispersed with a SPEX grating monochromator and detected with Hamamatsu photomultiplier tube R928. A pulsed nitrogen laser (4-ns pulses with repetition of 20 Hz and photon energy 3.68 eV) was used to determine the lifetime of the defect-related PL. Neutral density filters were used to attenuate the excitation density. The pump density was varied in the range of 10^{-5}–35 W/cm^2 for cw excitation, and 10–10^4 W/cm^2 in peak for pulsed excitation. The temperature of the samples was varied from 15 to 360 K using a closed cycle cryostat and from 300 to 600 K using a heating stage.

B. Low-temperature PL

Typical PL spectra for undoped GaN samples at 15 K in cw mode are shown in Fig. 3. In all of the studied samples, the PL spectrum involved the YL, BL, and SD-SA bands, and also the near-band-edge emission formed by the bound

TABLE I. Quantum efficiencies of different recombination channels in undoped GaN at 15 K.

	Directly measured $\eta_i(0)$					$\eta_i(0)$ calculated from Eq. (13)		
Sample	Exciton	SD-SA	BL	YL	Total	SD-SA	BL	YL
RK83	0.103	0.028	0.107	0.047	0.285		0.29	0.073
RK85	0.05	0.09	0.025	0.025	0.19	0.24		
RK93	0.17	0.045	0.22	0.095	0.53		0.37	0.083
RK120	0.1	0.003	0.07	0.11	0.283			0.14
RK170	0.18	0.003	0.23	0.08	0.493		0.227	0.08

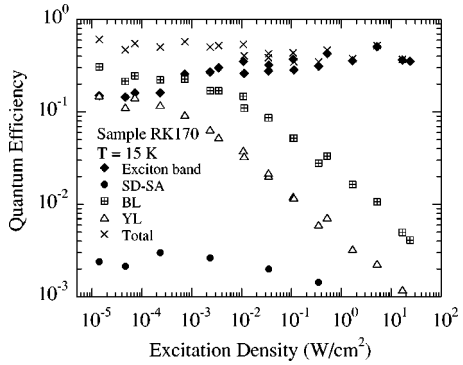

FIG. 4. Variation of quantum efficiency of different recombination channels with excitation intensity.

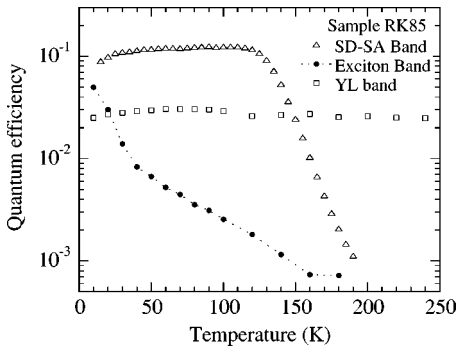

FIG. 6. Temperature dependencies of QE of the main PL bands in the sample RK85 at excitation density of 2×10^{-4} W/cm^2.

and free exciton transitions and their phonon replicas. The contribution of the defect-related bands varied in a large set of samples. We have chosen five samples with different intensities of PL bands for detailed study. The high quality of the samples was confirmed by a narrow full width at half maximum (FWHM) of the exciton line, 3–9 meV, as well as by the high QE of radiative emission, 10–50% in the low excitation limit for most of the samples (Table I). The QE of PL has been measured as a ratio of the integrated PL intensity to the intensity of the incident laser light with the correction for the geometry of the PL registration optics.[23] The values of QE estimated by this method will be compared below to the values obtained from the temperature dependence of PL intensity by the method described in Sec. II A. Variation of QE for each PL band with excitation density for one of the samples at low temperature is shown in Fig. 4. A decrease of QE for the defect-related bands and simultaneous increase of the exciton emission intensity is due to saturation of the hole capture by acceptors involved in PL, as described in Sec. II B.

C. Temperature dependence of PL intensity

The effect of temperature on the PL band intensities was studied at sufficiently low excitation intensity, so that the inequality $N_{Ai}^0 \ll N_{Ai}$ was valid for all acceptors under study. The temperature dependencies of the PL intensities for different bands were similar in all studied samples. The temperature dependence of the integrated PL intensity for the exciton emission (as a total emission in the range 3.3–3.5 eV), BL, and YL bands are shown in Fig. 5. The temperature dependence of the SD-SA band intensity is compared with the exciton emission and YL intensity in the sample with high QE of the SD-SA band in Fig. 6. It is seen that at temperatures from 15 to about 60 K a fast decrease of the exciton band intensity is accompanied by a corresponding increase in the defect-related PL intensity in accordance with Eqs. (5) and (6). In the temperature range 200–260 K, a quenching of the BL band, which has the highest QE in the sample RK170, is accompanied by an increase in intensity of the YL and exciton bands (the last is seen as a shoulder in Fig. 5). A slow decrease of the intensities of the YL and BL bands in the temperature regions between their enhancement and quenching (Fig. 5) will be discussed later.

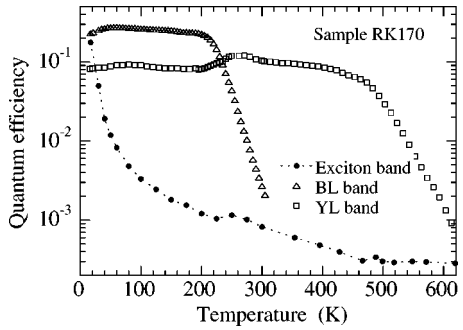

FIG. 5. Temperature dependencies of QE of the main PL bands in the sample RK170 at excitation density of 2×10^{-4} W/cm^2.

A similar increase of the YL band intensity in the temperature range 10–100 K has been observed in Ref. 24, which was attributed to the release of carriers from a level 13.7 meV below the shallow donor. Note that quenching of the integrated exciton emission in our sample similarly occurred with the activation energy of about 13 meV in this temperature range. It resulted in enhancement of other PL bands with similar activation energy, which is consistent with Eqs. (5) and (6). Therefore the ''unusual'' increase of the YL intensity observed in Ref. 24 is rather a consequence of a good quality of the sample (high radiative efficiency of exciton emission) and low excitation intensity conditions. We should emphasize that the enhancement of the PL intensity can be observed only at sufficiently low excitation intensities and in the samples with high radiative efficiency. We have estimated the QE for different PL bands from the values of steps in PL intensity by using Eq. (13). The obtained values, listed in Table I, demonstrate a rough agreement with the ''directly measured'' QE in these samples. The agreement supports in particular our assumption that the nonradiative recombination in the studied samples involves the capture of free carriers (rather than excitons) by deep nonradiative defects as discussed in Sec. II A.

D. Nonradiative capture of holes by acceptors

We have determined the hole-capture coefficients C_{pi} for the studied acceptors from the analysis of the quenching of the corresponding PL bands. In the first approximation we ignored the possible temperature-induced variation of param-

TABLE II. Characteristic lifetimes in the GaN samples.

	PL lifetime, τ_{Ri} (μs)			Hole capture time,[a] τ_i (ns), and τ^* (ns)			
Sample	SD-SA[b]	BL[c]	YL[d]	SD-SA	BL	YL	τ^*
RK83	1.8	7	40	2.2	0.64	1.4	0.068
RK85	2.7		37	0.62	2.6	2.8	0.056
RK93	2.5	9	60	2.5	0.64	1.4	0.14
RK120	2.4	15	52	35	1.8	1.1	0.13
RK170		13	56	43	0.43	0.8	0.1

[a]$T=15$ K.
[b]$T=110$ K.
[c]$T=200$ K.
[d]$T=300$ K.

eters η_i and C_{pi}. The values of τ_{Ri} have been obtained from the transient PL study at elevated temperatures close to the beginning of the quenching[25] (Table II). The temperature dependencies of the PL intensity in the quenching region for three PL bands in several samples are shown in Figs. 7, 8, and 9. From the fit to the experimental data, using Eqs. (5), (6), and (8)–(10), we have estimated parameters C_{pi}, σ_{pi}, and E_{Ai} for the studied acceptors (Table III). Note that the activation energies are close to those reported before[8–10] and the hole-capture cross section for the acceptor related to the YL is very close to the value found from the PICTS method (1.4×10^{-14} cm^2).[15]

E. Concentration of acceptors in GaN

After hole-capture coefficients are evaluated, the ratio between concentrations of each acceptor from an analysis of the low-temperature PL spectrum can be determined for each sample. This is a simple and effective method to estimate the relative concentration of uncontrolled acceptors in *n*-type GaN, which can be widely used for the sample characterization. Indeed, all that is necessary is to measure the PL spectrum at sufficiently low temperature and excitation intensity[26] and to find the integrated intensity of each band in relative units. Then the ratio between the concentrations of the ith and jth acceptor can be found from Eqs. (2) and (12) as

$$\frac{N_{Ai}}{N_{Aj}}=\frac{I_i^{\mathrm{PL}}}{I_j^{\mathrm{PL}}}\frac{C_{pj}}{C_{pi}}, \tag{28}$$

where the values of C_{pi} (C_{pj}) can be taken as average values listed in Table III.

To determine the absolute values of the acceptor concentrations, the concentration of one of the acceptors should be found independently by evaluation the dependence of the PL intensity on excitation intensity as described in Sec. II B. The generation rate of the photoexcited carriers, G, was calculated from the excitation density assuming that the effective thickness of the layer subject to excitation is 0.1 μm [0.07 μm is due to transmission with the absorption coefficient $\alpha=1.5\times10^5$ cm^{-1} at 325 nm (Ref. 27) and the rest was added to account for the hole diffusion]. In each of the samples, the dependencies were similar and one of them is shown in Fig. 10 as an example. A linear increase of the PL intensity is followed by saturation (after $G\approx10^{21}$ cm^{-3} s^{-1} or excitation density $\sim10^{-2}$ W/cm^2). A square-root dependence is observed for the higher generation rates. From the fit to the experimental data using both simplified expression (19) and exact solution of the system of Eqs. (20), (22), (23), (25) the concentration of acceptor responsible for the YL band has been estimated as shown in Fig. 10. Then, using Eq. (28), concentrations of two other

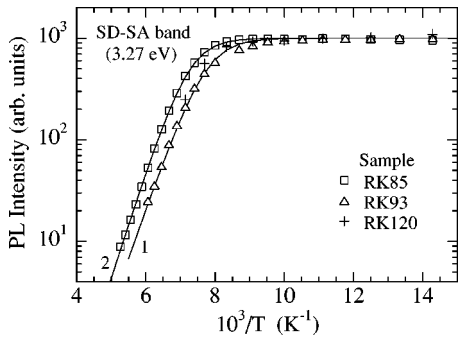

FIG. 7. Temperature-induced variation of the intensity of the SD-SA band in the region of its quenching. Solid curves demonstrate the best fit for the samples RK93 (1) and RK85 (2) by Eqs. (5), (6), and (8)–(10). The model parameters are listed in Tables II and III.

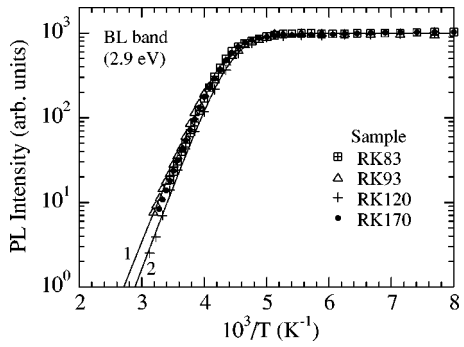

FIG. 8. Temperature-induced variation of the intensity of the BL band in the region of its quenching. Solid curves demonstrate the best fit for the samples RK93 (1) and RK120 (2) by using Eqs. (5), (6), and (8)–(10). The model parameters are listed in Tables II and III.

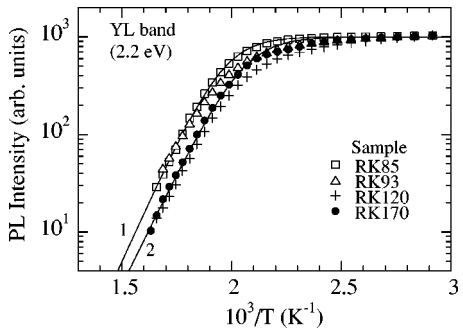

FIG. 9. Temperature-induced variation of the intensity of the YL band in the region of its quenching. Solid curves demonstrate the best fit for the samples RK85 (1) and RK170 (2) by using Eqs. (5), (6), and (8)–(10). The model parameters are listed in Tables II and III.

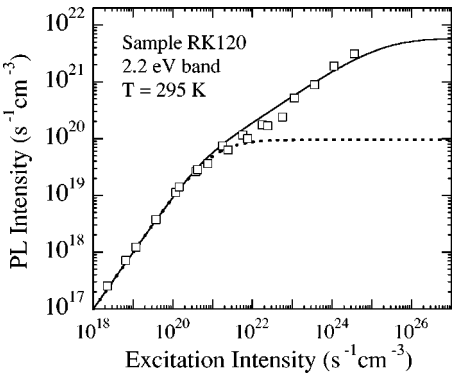

FIG. 10. Dependence of the YL intensity on excitation intensity for the sample RK120 at room temperature. Solid curve represents a fit with Eqs. (20), (22), (23), and (25) with the following parameters: $n_0=1.7\times10^{17}$ cm^{-3}, $N_{Ai}=5\times10^{15}$ cm^{-3}, $N_{DS}=10^{19}$ cm^{-3}, $C_{nS}=10^{-13}$ cm^3 s^{-1}, $C_{pS}=7\times10^{-10}$ cm^3 s^{-1}, $C_{ni}=1.13\times10^{-13}$ cm^3 s^{-1}, $C_{pi}=1.6\times10^{-7}$ cm^3 s^{-1}, $C_{\rm ex}=10^{-9}$ cm^3 s^{-1}. Note that $\tau_{Ri}=(C_{ni}n_0)^{-1}=52$ μs and $\eta_i=C_{pi}N_{Ai}(C_{pi}N_{Ai}+C_{pS}N_{DS}+C_{\rm ex}n_0)^{-1}=0.1$. Dotted line is a fit by Eq. (19) with the following parameters: $\eta_i=0.1$, $\tau_{Ri}=52$ μs, and $N_{Ai}=5\times10^{15}$ cm^{-3}.

acceptors have been calculated for the studied samples (Table IV). The resulting total concentration of acceptors is much less than the room-temperature concentration of free electrons in the studied samples. This result is consistent with the high mobility of electrons at room temperature (see Table IV).

The square-root dependence of the YL intensity on excitation power, observed in the high excitation region, can be explained by the presence of nonradiative deep donors N_{DS} in the studied samples. It is essential for the implementation of this model that $N_{DS}\gg n_0$. However, high electron mobility in our samples (Table IV) evidences that the concentration of the neutral donors cannot be higher than $\sim2\times10^{17}$–10^{18} cm^{-3}. To explain the discrepancy, we assume that nonradiative deep donors dominate near the sample surface and thus contribute much to the PL (PL is collected from about 0.1–0.3-μm-thick layer). At the same time, the Hall mobility of the 2-μm-thick GaN layer stays nearly unaffected by the presence of the deep donors in the surface layer.

F. Characteristic lifetimes in GaN

One can find the lifetime of the minority carriers (free holes) τ^* in these samples at low temperature. Rearranging Eqs. (2) and (17), one can obtain the expression for the lifetime:

$$\tau^*=\frac{\eta_i(0)}{C_{pi}N_{Ai}}, \tag{29}$$

where parameters $\eta_i(0)$, C_{pi}, and N_{Ai} are taken for any acceptor. The calculated values are shown in Table II [parameters $\eta_i(0)$ were taken from the direct measurement of QE for the dominant PL band in the sample, see Table I]. Characteristic times of the acceptor hole capture, obtained by using Eq. (16), are also shown in Table II.

Large difference between the hole-capture time and PL lifetime for all studied acceptors (Table II) confirms our previous assumption that the recombination rate through each channel is dictated solely by the hole-capture rate. Therefore the defect-related PL intensity is independent of both the luminescence lifetime and the transition mechanisms, such as DAP- or eA-type recombination as seen from Eq. (5) in the temperature range preceding PL quenching, where $\tau_{Ri}Q_i\ll1$ and $\tau_i\ll\tau_{Ri}$. Thus one should be careful in attempting to determine the transition mechanism from the

TABLE III. Parameters of radiative acceptors in undoped GaN found from the fit to experimental data using Eqs. (5), (6), and (8)–(10).

	C_{pi} (10^{-7} cm^3 s^{-1})			σ_{pi} (10^{-14} cm^2)			E_{Ai} (meV)		
Sample	SD-SA	BL	YL	SD-SA[a]	BL[b]	YL[c]	SD-SA	BL	YL
RK83		19			19.3			354	
RK85	10.5		7.7	14.4		6.4	181		888
RK93	9.3	2.9	0.4	12.8	3.0	0.3	167	318	755
RK120		7.3	1.6		7.4	1.3		343	775
RK170		6.8	3.5		6.9	2.9		344	830
Average	9.9	9.0	3.3	13.6	9.2	2.7	174	340	812

[a]$T=110$ K.
[b]$T=200$ K.
[c]$T=300$ K.

TABLE IV. Room-temperature Hall-effect data and concentration of radiative acceptors in GaN.

Sample	Hall-effect data at 295 K n_0 (10^{17} cm^{-3})	μ_n (cm^2 V^{-1} s^{-1})	Concentration of radiative acceptors (10^{15} cm^{-3}) SD-SA	BL	YL	Total
RK83	6.6	344	0.8	4	4	8.8
RK85	5.1	331	2.8	2	2	5.8
RK93	4.9	305	0.7	4	4	8.7
RK120	1.7	491	0.05	1.5	5	6.6
RK170	2.8	387	0.04	6	7	13.0

temperature dependence of PL intensity. Both mechanisms result in the same kind of the $I^{\mathrm{PL}}(T)$ dependence.

IV. DISCUSSION

A. Calculation of the capture cross section

In this section hole-capture coefficients are compared with the ones obtained from calculations made in the framework of the Ridley model for the capture rate involving the multiphonon process.[28] In this model the capture coefficient at reasonably low temperature can be expressed as[28]

$$C_{pi} \approx 2\pi\omega_0 C_0 V_T \frac{S^P \exp(-S)}{(P-1)!}[R_0 + (P-1)R_1], \quad (30)$$

where C_0 is the Coulomb factor, ω_0 is the effective phonon frequency, V_T is the volume of the localized state, S is the electron-phonon coupling strength (Huang-Rhys factor), P is the number of phonons emitted ($P = E_A/\hbar\omega_0$), and R_0, R_1 are numerical values of magnitude, respectively 0.26 and 0.18, and rather insensitive to other parameters. The Coulomb factor may be expressed as follows:[28]

$$C_0 = \frac{2\pi\mu}{1-\exp(-2\pi\mu)} \quad \text{with} \quad \mu = Z\sqrt{\frac{R_H^*}{E_{\mathrm{K}}}}, \quad (31)$$

where Ze is the charge of the acceptor, R_H^* is the effective Rydberg energy, and $E_{\mathrm{K}} \approx \frac{3}{2}k_B T$ is the kinetic energy of the hole in the valence band. For neutral centers C_0 is unity, for attractive centers $C_0 \approx 2\pi\mu$. We have estimated the volume of the localized state as $V_T = \frac{4}{3}\pi a_h^3$ with the radius of the bound hole a_h calculated in the effective-mass approximation[29] and listed in Table V. Parameters S, P, and $\hbar\omega_0$ are taken from Ref. 30 for the BL and YL bands (Table V). For the SD-SA band, it is reasonable to take $\hbar\omega_0 = 91$ meV since the coupling with the LO lattice phonons is strong for this band. The Huang-Rhys factor for this band can be found as a ratio between the intensities of the first phonon replica and the zero-phonon line.[14] The values of C_{pi} calculated using Eqs. (30) and (31) are shown in Table V in comparison with the experimentally found coefficients. Note that the expected values of C_{pi} for the attractive centers are quite close to those obtained from the experiment, yet the exact charge of the acceptors cannot be established from this comparison.

B. Variation of the capture coefficients with temperature

In the fitting of the $I^{\mathrm{PL}}(T^{-1})$ dependence by Eq. (5), only two variable parameters were used: C_{pi} and E_{Ai}. The hole capture coefficient C_{pi} determines the position of the quenching region, whereas the activation energy, E_{Ai} determines the slope of the $I^{\mathrm{PL}}(T^{-1})$ dependence in this region. Note that the possible temperature variation of C_{pi} does not affect the $I^{\mathrm{PL}}(T^{-1})$ slope. Indeed, in the region of thermal quenching, the following inequality is correct, $1 \ll (1-\eta_i)\tau_{Ri}Q_i$ in the denominator of Eq. (5), and the temperature dependence of C_{pi} is cancelled since both η_i and Q_i are proportional to C_{pi} [see Eqs. (2) and (8)]. Thus the values of the parameters C_{pi} and E_{Ai} are quite insensitive to the temperature, in the quenching region. In contrast, the temperature dependence of C_{pi} reveals itself in variation of $\eta_i(0)$ in the regions before quenching, where the Eq. (5) is simplified to $I^{\mathrm{PL}} \approx \eta_i(0)G$. The slow variation of quantum efficiency η_i with temperature can be caused not only by variation of C_{pi} of the analyzed center, but also by slow variation of $\Sigma_j C_{pj}$, see Eq. (2). Evidently, the temperature dependence of the capture rate of the dominant channel in the summation (nonradiative recombination channel in the analyzed samples) would cause the largest effect on the temperature dependencies of all radiative channels. Relatively small variation of I_i^{PL} with temperature in the regions between sharp quenching for the defect-related PL bands (see Fig. 5) may be related

TABLE V. Parameters used for calculation and the calculated values of the capture coefficients for the main radiative defects in undoped GaN. Experimental capture coefficients are shown for comparison.

Parameter	SD-SA band	BL band	YL band
a_h (Å)	5.0[a]	3.6[a]	2.4[a]
$\hbar\omega_0$ (meV)	91	43[b]	52[b]
S	0.5	3[b]	8[b]
E_{Ai} (eV)	0.174	0.34	0.81
P	2	8	16
$C_{pi}(Z=0)$ (10^{-7} cm^3 s^{-1})	0.3	0.079	0.061
$C_{pi}(Z=1)$ (10^{-7} cm^3 s^{-1})	5.5	1.1	0.67
$C_{pi}(Z=2)$ (10^{-7} cm^3 s^{-1})	11.0	2.1	1.3
Experimental C_{pi} (10^{-7} cm^3 s^{-1})	9.9	9.0	3.3

[a]Reference 29.
[b]Reference 30.

to a small temperature variation of the average hole-capture coefficient of nonradiative centers C_{pS}.

C. Identification of the radiative acceptors in undoped GaN

Analysis of the capture parameters shows that all three acceptors have large hole-capture cross sections. Similar value of the hole-capture coefficient (10^{-7}–10^{-6} $cm^3\,s^{-1}$) has been obtained for the acceptor responsible for the 1.2-eV band in *n*-type GaAs,[31] which was assigned to the Ga vacancy-shallow donor ($V_{Ga}D$) complex.[32] The charge state of the $V_{Ga}D$ complex in GaAs is either $1-$ (Ref. 33) or $2-$.[34] We assume that the acceptors responsible for the YL, BL, and SD-SA bands in *n*-type GaN also involve a gallium vacancy associated with different defects. Our results are consistent with the assumptions that relate YL and BL bands to the $(V_{Ga}D)^{2-}$ and $(V_{Ga}H)$ complexes.[10–13] Interestingly, it was suggested earlier that the shallow acceptor responsible for the SD-SA band is just V_{Ga},[35–37] however, such identification is inconsistent with much deeper energy-level position obtained for V_{Ga} from the first-principles calculations.[11,12] The exact microscopic origin of the acceptors in undoped GaN is the subject of future investigations.

V. SUMMARY

We have studied photoluminescence of the defect-related PL bands in undoped GaN as a function of temperature and excitation intensity. A general expression is obtained for the PL intensity of a given recombination channel in the presence of several PL bands. A general technique is developed to arrive at the acceptor concentrations responsible for these bands, quantum efficiencies and the lifetimes of minority carriers from the analysis of PL intensities at different temperatures and excitation intensities. The hole-capture cross sections for the acceptors responsible for the 2.2-, 2.9-, and 3.27-eV bands in undoped GaN are estimated from a PL study. The absolute values of the hole-capture cross section (10^{-14}–10^{-13} cm^2) indicate that these acceptors could be related to multiple negatively charged defects.

ACKNOWLEDGMENTS

The authors are grateful to Professor B. W. Wessels for the support and valuable comments. M.R. would like to thank also Professor A. A. Gutkin and Professor N. S. Averkiev for very helpful discussions. This work was supported by the NSF under grant ECS-9705134 and NASA under contract NAG5-8730.

*Present address: Department of Electrical Engineering, Virginia Commonwealth University, Richmond, VA 23284. Email address: mreshchi@saturn.vcu.edu

[1] E.F. Schubert, I.D. Goepfert, and J.M. Redwing, Appl. Phys. Lett. **71**, 3224 (1997).
[2] I.-H. Lee, J.J. Lee, P. Kung, F.J. Sanchez, and M. Razeghi, Appl. Phys. Lett. **74**, 102 (1999).
[3] R. Singh, R.J. Molnar, M.S. Ünlü, and T.D. Moustakas, Appl. Phys. Lett. **64**, 336 (1994).
[4] W. Grieshaber, E.F. Schubert, I.D. Goepfert, R.F. Karlicek, Jr., M.J. Schurman, and C. Tran, J. Appl. Phys. **80**, 4615 (1996).
[5] D.A. Turnbull, X. Li, S.Q. Gu, E.E. Reuter, J.J. Coleman, and S.G. Bishop, J. Appl. Phys. **80**, 4609 (1996).
[6] D.M. Hofmann, D. Kovalev, G. Steude, B.K. Meyer, A. Hoffmann, L. Eckey, R. Heitz, T. Detchprom, H. Amano, and I. Akasaki, Phys. Rev. B **52**, 16 702 (1995).
[7] J. Krüger, D. Corlatan, C. Kisielowski, Y. Kim, R. Klockenbrink, G.S. Sudhir, M. Rubin, and E. Weber, Mater. Sci. Forum **258-263**, 1191 (1997) (Trans. Tech. Publications, Switzerland, 1997).
[8] T. Ogino and M. Aoki, Jpn. J. Appl. Phys., Part 1 **19**, 2395 (1980).
[9] R. Dingle and M. Ilegems, Solid State Commun. **9**, 175 (1971).
[10] M.A. Reshchikov, F. Shahedipour, R.Y. Korotkov, M.P. Ulmer, and B.W. Wessels, J. Appl. Phys. **87**, 3351 (2000).
[11] J. Neugebauer and C.G. Van de Walle, Appl. Phys. Lett. **69**, 503 (1996).
[12] T. Mattila and R.M. Nieminen, Phys. Rev. B **55**, 9571 (1997).
[13] C.G. Van de Walle, Phys. Rev. B **56**, R10 020 (1997).
[14] A.M. Stoneham, *Theory of Defects in Solids* (Clarendon Press, Oxford, 1975).
[15] A.Y. Polyakov, N.B. Smirnov, A.V. Govorkov, M. Shin, M. Skowronski, and D.W. Greve, J. Appl. Phys. **84**, 870 (1998).
[16] K.D. Glinchuk and A.V. Prokhorovich, Phys. Status Solidi A **29**, 339 (1975); K.D. Glinchuk, A.V. Prokhorovich, and V.I. Vovnenko, *ibid.* **34**, 777 (1976).
[17] A.A. Gutkin, M.A. Reshchikov, and V.E. Sedov, Fiz. Tekh. Poluprovodn. **31**, 1062 (1997) [Sov. Phys. Semicond. **31**, 908 (1997)].
[18] M. Leroux, N. Grandjean, B. Beaumont, G. Nataf, F. Semond, J. Massies, and P. Gibart, J. Appl. Phys. **86**, 3721 (1999).
[19] Note that Eq. (1) remains valid if some defects are deep donors, not acceptors. One should just replace N_i^0 and N_i^- with N_i^+ and N_i^0, respectively, for such defects.
[20] O. Brandt, J. Ringling, K.H. Ploog, H.-J. Wünsche, and F. Henneberger, Phys. Rev. B **58**, R15 977 (1998).
[21] F. Binet, J.Y. Duboz, J. Off, and F. Scholz, Phys. Rev. B **60**, 4715 (1999).
[22] Solution of equations presented in Ref. 4 with the used parameters leads to the nine orders of magnitude different value of the critical generation rate compared to what follows from Fig. 5(a) of Ref. 4.
[23] For the setup calibration we used a Mg-doped GaN sample with very high radiative efficiency. The incident unfocused laser beam was absorbed in the thin surface layer of the sample. PL density was measured after the collimating lens with a calibrated power meter. It was compared with the incident laser power with correction for losses due to reflections and absorption by lenses and window. We assumed that PL, emerging from the thin surface layer of GaN sample, propagates in all directions and refracts at the GaN-vacuum interface according to the different refraction indexes. According to our estimates, a lens with a diameter of 5 cm located at the distance of 15 cm from the sample collected about 1/1000 of the total PL. The internal QE of the most efficient GaN:Mg sample approached the unity.
[24] R. Seitz, C. Gaspar, T. Monteiro, E. Pereira, M. Leroux, B. Beamont, and P. Gibart, MRS Internet J. Nitride Semicond. Res. **2**, 36 (1997).

[25] It has been established that in a wide temperature range before the quenching the PL decay was nearly exponential for all three acceptors and the characteristic lifetime was nearly independent of temperature.

[26] The temperature should be low enough that the considered PL bands do not quench, and the excitation should be chosen below the saturation region.

[27] G. Yu, G. Wang, H. Ishikawa, M. Umeno, T. Soga, T. Egawa, J. Watanabe, and T. Jimbo, Appl. Phys. Lett. **70**, 3209 (1997).

[28] B.K. Ridley and M.A. Amato, Solid State Phys. **14**, 1255 (1981); B. K. Ridley, *Quantum Processes in Semiconductors* (Clarendon Press, Oxford, 1999), Chap 5.

[29] R.Y. Korotkov, M.A. Reshchikov, and B.W. Wessels, Physica B **273-274**, 80 (1999).

[30] M.A. Reshchikov, F. Shahedipour, R.Y. Korotkov, M.P. Ulmer, and B.W. Wessels, Physica B **273-274**, 103 (1999).

[31] V.I. Vovnenko, K.D. Glinchuk, K. Lukat, and A.V. Prokhorovich, Fiz. Tekh. Poluprovodn. **14**, 1003 (1980) [Sov. Phys. Semicond. **14**, 596 (1980)].

[32] E.W. Williams, Phys. Rev. **168**, 922 (1968).

[33] D.T.J. Hurle, J. Appl. Phys. **85**, 6957 (1999).

[34] N.S. Averkiev, A.A. Gutkin, E.B. Osipov, M.A. Reshchikov, and V.R. Sosnovskii, Defect Diffus. Forum **103-105**, 31 (1993).

[35] T.L. Tansley and R.J. Egan, Phys. Rev. B **45**, 10 942 (1992).

[36] M. Ilegems, R. Dingle, and R.A. Logan, J. Appl. Phys. **43**, 3797 (1972); M. Ilegems and R. Dingle, *ibid.* **44**, 4234 (1973).

[37] P. Boguslawski, E.L. Briggs, and J. Bernholc, Phys. Rev. B **51**, 17 255 (1995).